Dielectric, Magnetic and Surface Analytical Study of Dy and Tb Doped (Bi, Pb)(Fe,Ti)O_3 Multiferroic Ceramics

Monika Mishra[1*], Javalkar Dinesh kumar[2], Ritu Sindhu[3]

[1*]Research Scholar, Department of Physics, School of Basic & Applied Sciences, Lingaya's Vidyapeeth, Greater Faridabad, Haryana, India
[2]Associate Professor, Department of Electronics & Electrical Engineering, Lingaya's Vidyapeeth,Greater Faridabad, Haryana, India
[3]Senior Professor, School of Computer Science & Information Technology, Lingaya's Vidyapeeth, Greater Faridabad, Haryana, India

Abstract: Polycrystalline samples of $Bi_{0.8}A_{0.1}Pb_{0.1}Fe_{0.9}Ti_{0.1}O_3$(where A = Dy and Tb) ceramics have been prepared through high temperature sintering technique. X-ray diffraction analysis showed that the ceramics possess perovskite phase with hexagonal crystal symmetry. Dielectric and electrical properties indicate that the Curie temperature shifted to higher temperature with Dy doping. AC conductivity of the sample increases with increase in temperature which confirms the negative temperature coefficient of resistance (NTCR) behaviour of material. Substitution of Dy and Tb ions at A-site suppress the spiral spin structure of $BiFeO_3$ which is further responsible for the appearance of weak ferromagnetism atroom-temperature.Induced destruction of the spin cycloid due to the Dy and Tb substitution, these multiferroic properties are attributed because of the enhanced magneto-electric interaction.

Keywords: Ferroelectric; Ceramics; Multiferroics, Perovskite, Dielectric, Impedance, NTCR

1. Introduction

Multiferroics have simultaneous electric and magnetic ordering, thereby also referred to ferroelectromagnets (FM), magneto-electrics(ME) and/or ferroelastics. These multiferroics have gained much attention for their potential applications and rich fundamental physics. Magneto-electric effect denotes the coupling betweenthe magnetic and the electric properties of a material. The small coupling between the electric and magnetic properties of the system in multiferroic provides an additional degree of freedom for device fabrication**[1, 2**]. $BiFeO_3$(BFO) and $Bi_5FeTi_3O_{15}$ (BFTO) are few such examples of multiferroic systems **[3, 4**]. The ferro-electromagnetic property of sulphide spinels and oxide perovskites have been also reported [**5**]**.**Those materials possessing ABO_3type structure offers a broad range of magnetic and electrical properties which mainly coversanti-ferroelectric, anti-ferromagnetic propertiesin metals, semiconductor, and insulator. Hence by making acomposition of these perovskite materials opens new ways to achieving the multiferroic properties in a single phase system. In latest researches, several composite groups for the synthesis and characterization of multiferroic perovskite systems such as [$BiFeO_3$ (BF) – $BaTiO_3$ (BT)]anti-ferromagnetic-ferroelectric[6], anti-ferromagnetic/weak ferromagnetic–ferroelectric [(BF)–$PrFeO_3$(PF)–$PbTiO_3$ (PT)[7] and $BiDyFeO_3$ (DF)–$BaTiO_3$ (BT)] systems have also been reported [**8**].

As per the intensively reported studies in recent years, $BiFeO_3$ has come out to be a perovskite structure exhibiting several magneto-electric properties at room temperature. BFO is a ferroelectric material with a Curie temperature of about 1103 K and anti-ferromagnetic with a Neel temperature (T_N) of 643 K [**9**]. $BiFeO_3$ has been synthesized by deploying several synthesis techniques such solid state, sol gel method and hydrothermal process etc. In the solid state technique, Bi_2O_3 and Fe_2O_3 are made to react within the temperature range of 800–830 ^{0}C and the remaining unreacted secondary phases Bi_2O_3/$Bi_2Fe_4O_9$ phases are removed by washing with HNO_3. The disadvantage of this process is that there is the necessity of leaching the unwanted phases during synthesis by using an acid and effectively providing the coarser powder& reproducibility of the process is also poor[**10**]. To synthesize pure $BiFeO_3$, some attempts were already madebut small traces of $Bi_{46}Fe_2O_{72}$ was found while the sintering of ceramics is done[**11**]. Therefore, utilization of $BiFeO_3$-ABO_3 solid solution systems is one of the ways to increase the sinterability and stability of structure of composite material. Moreover, another major issue reported forBFO-based ceramics is that their insulating resistance is very low which creates difficulty inmeasurements of ferroelectric, dielectric quantity and magneto-electric coupling at room temperature.

RMO_3 (where R is a rare-earth ion and M is a transition metal atom), $DyFeO_3$and $TbFeO_3$also belong to this class of perovskite oxides. Just like $BiFeO_3$, $DyFeO_3$is also having centre of inversionexhibiting orthorhombic structure [**12**]. Magnetic field induced ferro-electricity in $DyFeO_3$and $TbFeO_3$crystal can be controlled by magnetic field and the ferroelectric state can be reversible by varying the material in magnetic field which confirms the strong magneto-electric coupling present in such systems[**13**]. Ferro electricity was also induced in these systems by epitaxial strain due to the result of structural distortionin the structures of multiferroic systems[**14**]. Solid solution of bismuth ferrite and rare earth ferrites strongly infers the several interesting properties for magneto-electric applications. Because of the high electric conductivity of $BiFeO_3$, synthesis of pure polycrystalline sample of $BiFeO_3$(BFO)isquite challengingbecause there is always theformation of

secondary stable thermodynamically phase of $Bi_2Fe_4O_9$. Other ferroelectrics such as $PbTiO_3$ with perovskite structure were introduced to form solid solutions with $BiFeO_3$in order to stabilize the perovskite phase. $PbTiO_3$also helps in reducing electrical coercive fieldby forming a morphotropic phase boundary (MPB) with $BiFeO_3$[15]. Phases of different symmetries are separated by this morphotropic phase boundary (MPB) arising from $PbTiO_3$ and $BiFeO_3$ sides[16, 17]. Structural, magnetic and morphological propertiesas a function of composition of (1-y)($BiFeO_3$)-y($PbTiO_3$) solid has been reported by many researchers. Investigations revealedthat availability of mixed crystals with a $BiFeO_3$-$PbTiO_3$ (BF-PT) in ratio of 50:50 ultimately favours the formation of chemically ordered micro-regions where the spiral spin modulation is found to be decreased[18]. In addition to this, it was observed that the substitution of Ti at B-atomic site i.e. in place of Fe results in increase in magnetic properties ofcompounds[19, 20].Hence, the overall magnetic behaviour of bulk $REFeO_3$ (RE-Rare Earth)can besummed up the as the result of two contributing magnetic 'sub lattices': (i) an antiferromagnetic iron oxide lattice in which the spins are coupled through a Fe^{3+}–O^{2-}−Fe^{3+}super exchange mechanism; and (ii) a paramagnetic contribution which are due to essentially non-coupled ions. A small ferromagnetic moment is observed in the iron containing sub lattice due to spin-canting. Spin canting is a phenomenon through which the spins are tilted by a small angle about their axis. This ferromagnetic moment is observed because of the distortion caused inperovskite structure in one particular crystallographic direction[21]**.** In this study, the investigations of the crystal structure, dielectric and magnetic properties of the ternary perovskite system $Bi_{1-x}A_xPb_yFe_{1-y}Ti_yO_3$ (where A = Dy, Tb, x=0.1 and y=0.1) (which is a combination of three ternary perovskite, Ferroelectric and Ferromagnetic) have been carried out. Radii of Dy and Tb are just similar to each other (Atomic radii ofTb = 225pm and Dy = 228pm) and used to substitute at the A site of samples which further helps in decreasing the amount of oxygen vacancies and Bi volatilization.

2. Experimental procedure

Polycrystalline samples of $Bi_{0.8}A_{0.1}Pb_{0.1}Fe_{0.9}Ti_{0.1}O_3$(BPFT) (A = Dy and Tb) were synthesized from high purity oxides (Bi_2O_3 (Aldrich chemicals USA), Fe_2O_3 (Aldrich chemicals, USA), Dy_2O_3 (M/S Aldrich chemicals, USA), Tb_4O_7 (M/S Aldrich chemicals, USA), PbO (M/S Aldrich chemicals, USA) and TiO_2, (Aldrich chemicals, USA), through high temperature solid-state methodology. The reagentsof sample compounds were mixed in a unit of ball milling machinethoroughlyfor almost around 48 hours takenin suitable stoichiometry. The powder was first kept for dryingcompletelyat temperature 125 °C in order to remove its moisture. Before being cold pressed, the powder is calcinedat 800 °C in alumina cruciblesfor a time period of around 4 hours. Then a hydraulic press is used to makecylindrical pellets of the calcined fine powder, pressed with a pressure of 50MPa to make pellets of order of 10 mm in diameter and 1-2 mm in thickness. These pellets wereembedded in the same composition then sintered at 850°C for 4-5 hours. The XRD patterns were recorded atroom temperature using X-ray powder diffractometer (RigakuMinifiex, Japan) with CuKα radiation of wavelength (λ = 1.5405 Å)at a scanning rate of around 1/2° min^{-1} in a wide range of Bragg angles 2θ (20° ≤ 2θ ≤ 60°)to confirm the pure phase formation and compound quality at room temperature.The sintered pellets were firstly ground and then polished with silver paste on opposite faces of coated pellets beforemaking the dielectric measurements.The value of dielectric constant (ε) and loss tangent (tanδ) of the compounds were also calculated (RT) and as a function of frequencyin ahome-based furnacewithin a frequency range of (10^2-10^6Hz)in a temperature range of RT -400 ˚Cusing a HP 4284A Precision LCR meter. The magnetic studies were recorded by deploying Cryogenicvibrating sample magnetometer (VSM).

3. Resultsand Analysis

3.1. Phase and structural characterization

The XRD patterns of ($Bi_{0.8}A_{0.1}Pb_{0.1}Fe_{0.9}Ti_{0.1}O_3$ (A = Dy and Tb) ceramics at room temperature is given in **Fig. 1a**. It is observed thatall the samples have a single phaseat room temperatureand exhibits a hexagonal structure (JCPDS#742497 $Bi_{0.8}Pb_{0.2}Fe_{0.8}Ti_{0.2}O_3$).Anobserved inter-planar distance **d** is marked and further used to index all the reflection peaks of compounds (**Table 1**). Least-squares refinement method is performed to evaluate the lattice constants of $Bi_{0.8}A_{0.1}Pb_{0.1}Fe_{0.9}Ti_{0.1}O_3$. The observed and calculated **d** values of all diffracted lines (reflections) of the above compounds strongly indicated thatas we increase or decrease the doping concentration in compound, nochange in the parenthexagonalstructure of crystal.During synthesis,BFO is found to compose of two or more distinct phases one is dispersed phase along with matrix phase impuritybecause of the kinetics of the formation, The observed impurity phase attributed tothe presence of $Bi_2Fe_4O_9$(Secondary phase) is shown as in **Fig. 1a.** When we move from Dy doped BPFT to Tb doped BPFT, this secondary phase is disappeared.As it is discussed for $BiFeO_3$, it has never beenan easy task to synthesize a pure quality compound of BFO. Reported studies revealed thatthere is always a small concentration of impurity presentalong with major phase.[22].**Fig. 1b** shows the (020) and (120) diffraction peaks of the compounds which confirm no peak shifts has been occurred. The intensity increases as we move from Dy doped BPFT to Tb doped BPFT which is due to the substitution ofthese ions at Aatomic sites.

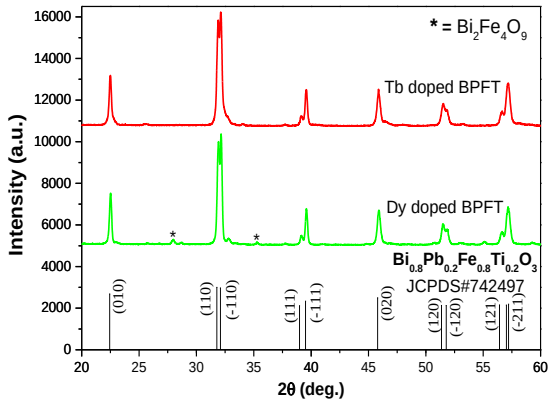

a

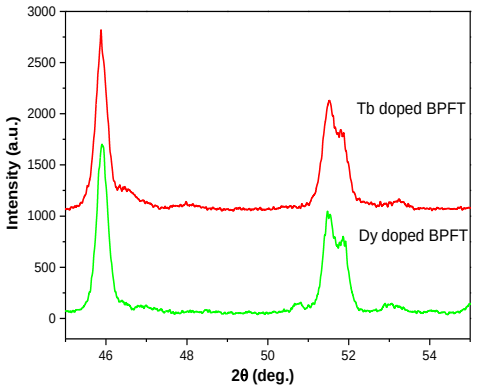

b

Fig. 1(a) *XRD patterns of $Bi_{0.8}A_{0.1}Pb_{0.1}Fe_{0.9}Ti_{0.1}O_3$samples)at Room temperature with different rare earth metal doping(A = Dy and Tb) (b) the broadening of (020) and(120) peaks.*

Table 1:Lattice parameters of Dy and Tb doped $Bi_{0.8}A_{0.1}Pb_{0.1}Fe_{0.9}Ti_{0.1}O_3$ceramics.

Sample	Crystal System	Particle size	Lattice Parameter	d_{obs}	d_{cal}	Hkl
BDPFT BTPFT	Hexagonal	~30-40nm	a = 5.5728Å c = 6.9257Å	3.9586	3.9596	(010)
				2.8133	2.8135	(110)
				2.7868	2.7864	(-110)
				2.3081	2.3085	(111)
				2.2789	2.2787	(-111)
				1.9799	1.9798	(020)
				1.7775	1.7777	(120)
				1.7640	1.7640	(-120)
				1.6295	1.6297	(121)
				1.6137	1.6139	(-121)
				1.6088	1.6087	(-211)

3.2. Dielectric properties

As well known, the Dielectric constant is inversely proportional to temperature.**Fig. 2 a, b** shows the variation of dielectric constant (ε) and tanδwith temperature for both compositionsbetween the frequency range of 10 kHz and 100 kHz.The presence of these two phases confirms the presence of two different ferroelectric compounds i.e. $BiFeO_3$ and $PbTiO_3$in the ceramic system [24-26].Ferroelectric-ferroelectric phase transition is indicated byfirst and second peak which correspond to the ferroelectric–paraelectric phase transition [23]. As observed at both the frequencies (10 kHz and 100 kHz), the value ofTb doped BPFT is much larger than the dielectric constant of Dy doped BPFT. In **Fig. 2b**, it is represented that up to 275 ^{0}C, the dielectric loss gradually increasesin a smooth manner. Doping effect is contributed by even very small impurities segregated to boundaries. Thesedoping may cause the transformation of dielectric into a semiconductor. So, the problem of synthesizing pure BFO still persists as there is spontaneous change of the oxidation state of Fe^{3+}/Fe^{2+}[27, 28].

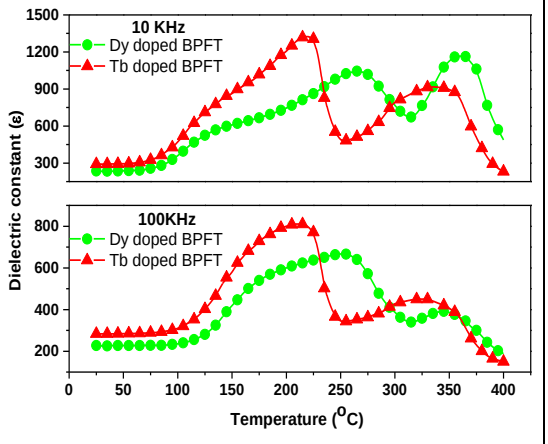

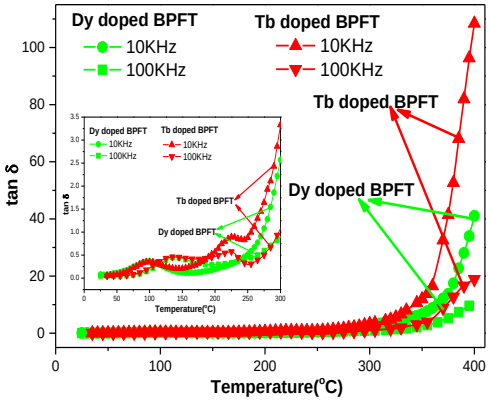

Fig.2(a)*Variation of dielectric constant (ε) and (b) loss tangent (tan δ) of Dy and Tb doped* $Bi_{0.8}A_{0.1}Pb_{0.1}Fe_{0.9}Ti_{0.1}O_3$*ceramics with Temperature at frequency 10 kHz and 100 kHz.*

Above Curie temperature, the dielectric permittivity of an ideal ferroelectric follows the Curie-Weiss law given in **Eq. (1),**

$$1/\varepsilon = (T-\theta)/C,\ (T>\theta) \quad \text{.....Eq. (1)}$$

Where C is Curie-Weiss constant, θ represents Curie-Weiss temperature. It is observed in the paraelectric phase only at blocking Temperature (T_B). **Fig. 3a-b** shows the inverse of ε as a function of temperature at 10 kHz & 100 kHz and the fitting of the experimental data to Curie-Weiss law. From the figure, a deviation from Curie-Weiss law starting at $T_B$has been observed. The parameter ΔT_m is often used to show the degree of deviation from the Curie-Weiss law. ΔT_m is the temperature where the ferroelectric transition can occurdefined by$\Delta T_m = T_B - T_m$. T_B is determined from the Curie-Wiess law[29].

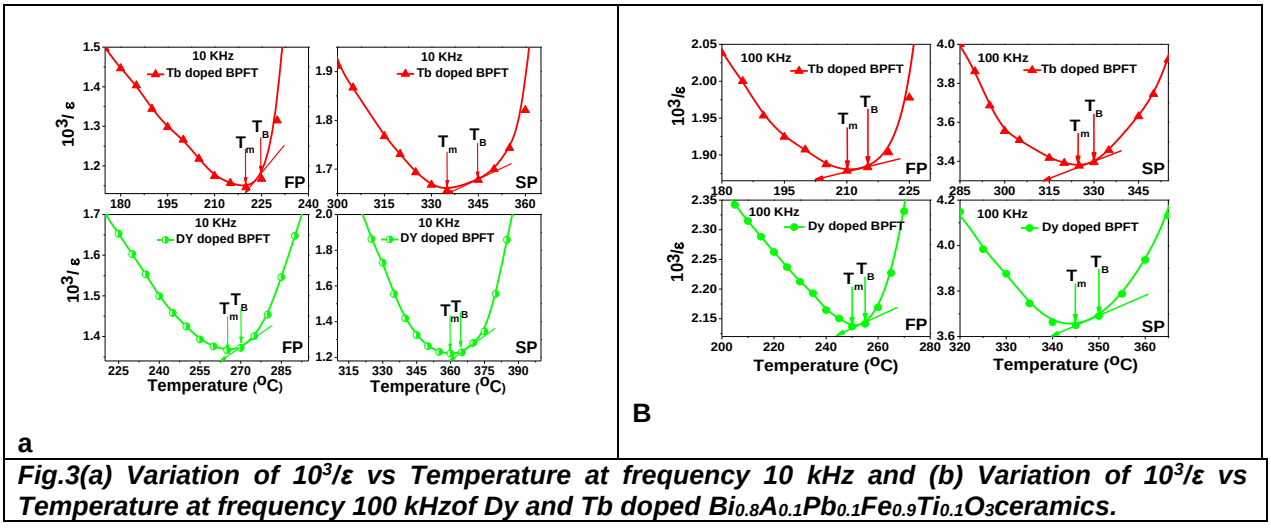

Fig.3(a) Variation of $10^3/\varepsilon$ vs Temperature at frequency 10 kHz and (b) Variation of $10^3/\varepsilon$ vs Temperature at frequency 100 kHzof Dy and Tb doped $Bi_{0.8}A_{0.1}Pb_{0.1}Fe_{0.9}Ti_{0.1}O_3$***ceramics.***

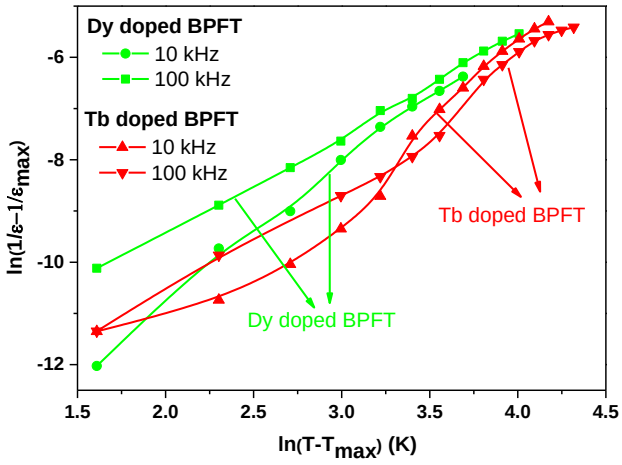

Fig.4. Variation of ln(1/ε- 1/ ε_{max}***) vsln(T-*** T_{max}***) of Dy and Tb doped*** $Bi_{0.8}A_{0.1}Pb_{0.1}Fe_{0.9}Ti_{0.1}O_3$***ceramics at frequency 10 kHz and 100 kHz respectively.***

Fig.4. representsvariation of ln(1/ε- 1/ε_{max}) vsln(T-T_{max}) of Dy and Tb doped $Bi_{0.8}A_{0.1}Pb_{0.1}Fe_{0.9}Ti_{0.1}O_3$ceramics at frequency 10 kHz and 100 kHz respectively.The graphs betweenlog σ_{ac} $(\Omega cm)^{-1}$Vs $10^3/T$ (K^{-1}) of Dy doped BPFT and Tb dopedBPFT at frequency 10 kHz and 100 kHzin the temperature range from 320^0C to 400^0C are drawn and given in **Fig. 5.** Impedance data collected from the LCR meter. The AC electrical conductivity was calculatedusing the formula:

$$\sigma = \omega\varepsilon\varepsilon_o tan\delta$$

Where ω is the angular frequency, ε is the vacuum dielectric constant, and k_B is the Boltzmann constant. At Curie temperature(Tc), there is usual change in slope only at higher frequencies is observed.Activation energy was calculated by using the slope of ln(σ_{ac}) vs $10^3/T$ inparaelectric regionby using the conductivity relation $\sigma = \sigma_o exp(-E_a/k_BT)$[30].

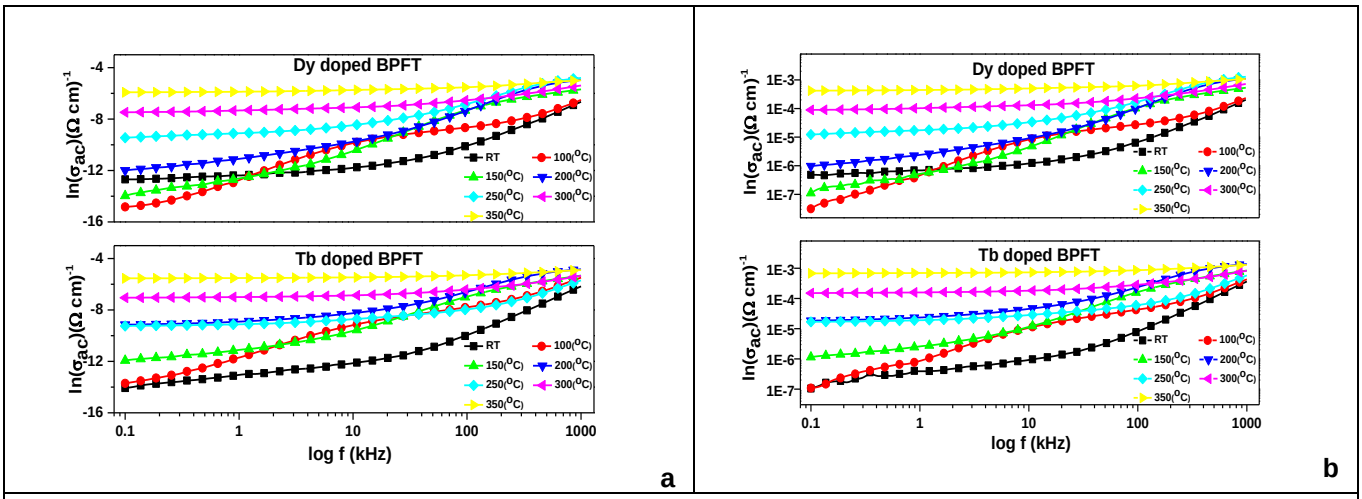

Fig.5(a)Variation of lnσ$_{ac}$ (Ωcm)$^{-1}$ vs. frequency and (b) Variation of lnσ$_{ac}$ (Ωcm)$^{-1}$ vs. frequency (through R) of Dy and Tb doped Bi$_{0.8}$A$_{0.1}$Pb$_{0.1}$Fe$_{0.9}$Ti$_{0.1}$O$_3$ceramics at different temperatures.

Thevalue of activation energy is indexed in **Table 2**.

Table 2: Details of the physical parameters ofDy and Tb doped BPFT ceramics

Sample Name	Frequency(kHz)	T^1_{max}	ε^1_{max}	T^2_{max}	ε^2_{max}	γ	Ea(eV)
BDPFT	10	265	1044	360	1168	1.9496	0.34
	100	250	667	345	390	2.7090	0.15
BTPFT	10	220	1330	335	920	2.3096	0.43
	100	210	811	325	451	2.7032	0.29

The frequency spectrum of the conductivity at different range of temperatures for the samples is shown in **Fig. 6**. Low frequency dispersion obeying the power law feature (Joncher law) has been observed tochange its slope governed by n. At higher frequency, the hopping takes place by charge carriers through trap sites that minimsize the effects of unintentional interference.The conductivity is lower at low frequency which is attributed because of thenumbers of charge carriers which have high relaxation time due to higher energy barriers respond in low frequency region might be less in numbers. The potential height is reduced as the thermal energy of the charge carriers is increased at higher temperatures. A low frequency dispersion region is shown by the conductivity spectrum which is further followed by a high frequency plateau region. DC conductivity is caused by the frequency independent plateau region and low frequency region corresponds to the AC-conductivity. Due to presence of space charge, the dispersion behaviour may be observed while the space charge becomes less activein the plateau region at higher frequency domain. At lower temperatures σ_{ac} linearly varies with frequency and non-linearity occurs in the high frequency region. This behaviour indicates the role of hoppingphenomenonis so prominent in conduction process at low temperature region.

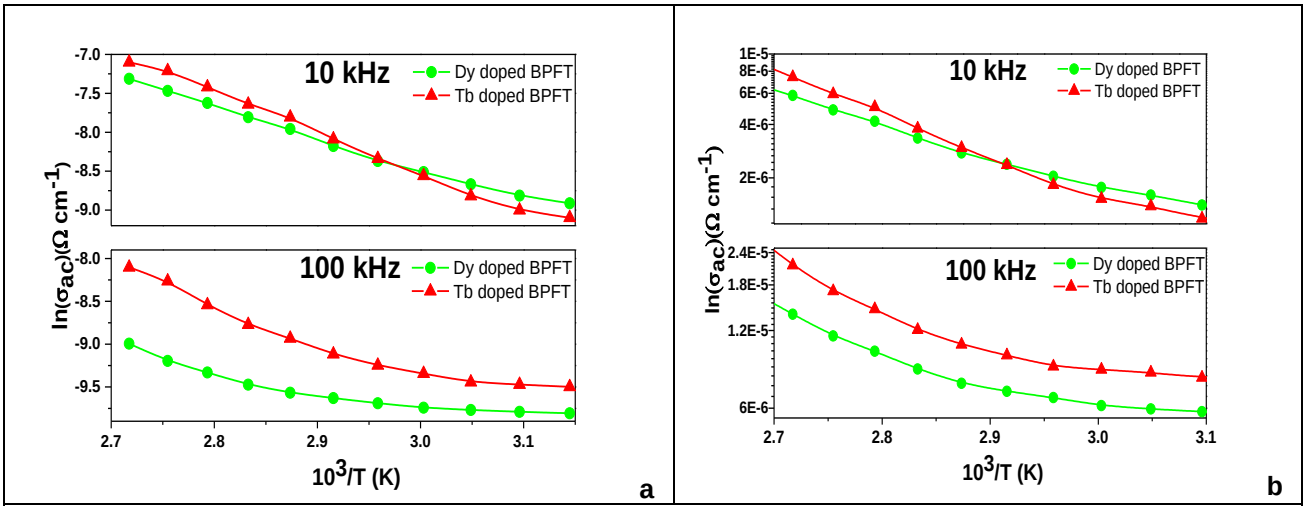

Fig.6(a)Variation of lnσ$_{ac}$ (Ωcm) vs 10^3/T and (b) Variation of lnσ$_{ac}$ (Ωcm) vs 10^3/T (through R) of Dy and Tb doped Bi$_{0.8}$A$_{0.1}$Pb$_{0.1}$Fe$_{0.9}$Ti$_{0.1}$O$_3$ceramics at frequency 10 kHz and 100 kHz.

3.3. Magnetic properties

Fig. 7is showing the magnetic moment as a function of temperature under zero-field cooled (ZFC) and field cooled (FC) conditions with an applied magnetic field of 1 Teslabetween 5 and 300 K. By cooling the sample in zero-field, then warming within the field of 1 Tesla and simultaneously measuring the magnetization while increasing the temperature (from RT- 5 K,) the field cooled (FC) magnetization isobtained. Here, the transition temperature is defined as the temperature at which the Zero Field Cooled (ZFC) and Field Cooled curves (FC) get bisected. From the figure 6, it has been concluded that on increasing the temperature, initially the value ofZFC magnetization increases, reaches its maximum and then decreases atblocking temperature (T_B) which is defined as the temperature at which the nano-particle moment gets blocked (do not relax). Below this T_B, the material shows the slow rate of relaxation of magnetization. These spins can flip only above this Blocking temperature(T_B). The Zero Field Cooled(ZFC) magnetization coincides with the Field Cooled(FC) magnetization at this point. The magnetic moment (M) vs. temperature (T) curves of Dy doped BPFT and Tb doped BPFT samples under the ZFC and FC has been presented which shows a systematic change under specific conditions.The highvalue of magnetization at the low temperature range strongly infers that there is presence of uncompensated anti-ferromagnetic spins (Fe^{3+}). As shown in **Fig. 7**, initially the value of saturated magnetization decreases with anincrease in temperatureand then increases This behaviour is attributing the presence of either some paramagnetic spins that are not depending upon the anti-ferromagnetic ordering or uncompensated magnetic spins, which results in superparamagnetic ordering as in case of anti-ferromagnetic domains[24, 31, 32].In this phenomenon,the magnetic materials showing the properties similar to that of paramagnetism even when the temperatures are below the Curie temperature or the Neel temperature. The phenomenon, where the energy required to change the direction of the magnetic moment of a particle is comparable to the ambient thermal energy, is a small length-scale phenomenon. The rate at which the particles randomly reverse their direction becomes significant at this point. The anomalous magnetization could be affected by the fluctuation of Fe valance ions that goes from 3^+ to 2^+. The variation of M–T curves with doping composition might be due tothereduction in particle size, doping at A and B sites, variation in the oxygen stoichiometry and due to the change in the magnetic anisotropy[33].

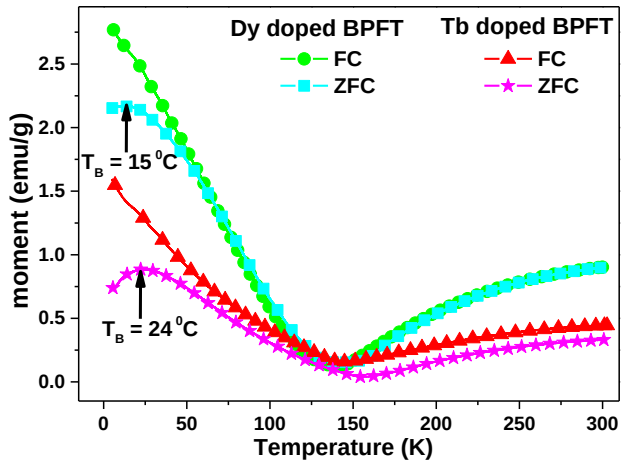

Fig.7 Variation of magnetization FC and ZFC of Dy and Tb doped $Bi_{0.8}A_{0.1}Pb_{0.1}Fe_{0.9}Ti_{0.1}O_3$ceramics with temperature (K).

Theset of magnetization curves known asM-H hysteresiscurves of ferromagnetic material measured at temperatures 5 K and 300 K is shown in **Fig. 8.**The Magnetic-Hysteresisloops depicts thatthe magnetization curves of the loop at low field are not collinear hence the samples is a weak ferromagnetic material. **Fig. 8**confirms theferromagnetic nature of sampleas there is nonzero remnant magnetization and coercivity as shown in the partly enlarged curves. In these samples,anincrement of magnetization is observed which is always ascribed because of theincomplete rotation of the spins along the direction of the wave vector i.e. size effects of the suppression of helical order hence contribute for increase in spin canting due to surface strain and oxygen defects[34, 35]. The net magnetization will be enhanced by the uncompensated spins and this cycloid spin structure could be suppressed, the canting of spin due to surface strain as well[36]. On the other hand, magnetization could be increased by oxygen defects as they introduce Fe^{2+} into the ferromagnetic order across Fe^{3+}–O^{2-}–Fe^{2+}[34, 37]**.**During the high temperature annealing process,the canting angles in samples were modulated because of the interaction between the external magnetic field and the uncompensated spins in the canted anti-ferromagnetic order. This modulation of canting angles is assumed to be one of the causesfor the increase in net magnetization of the sample.

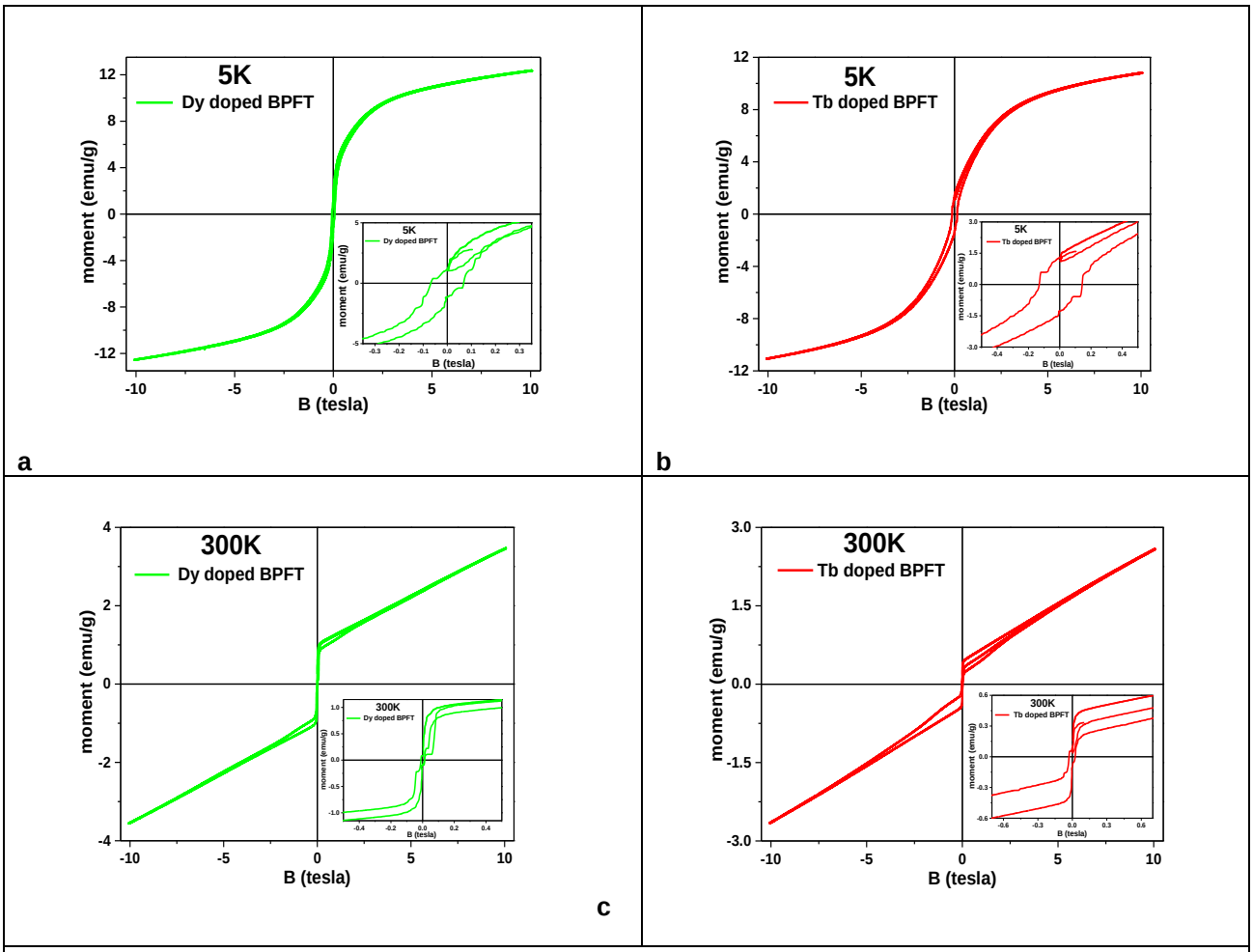

Fig.8 M–H loops of Dy and Tb doped $Bi_{0.8}A_{0.1}Pb_{0.1}Fe_{0.9}Ti_{0.1}O_3$ceramics at (a) 5 K and (b) 300 K.

The effect of doping on saturated magnetization is given in **Fig. 9.** Both magnetic hysteresis loops are measured at temperature range of 5 K and 300 K which shows that value of saturated magnetization is higher forDy doped BPFT than that of Tb doped BPFT.

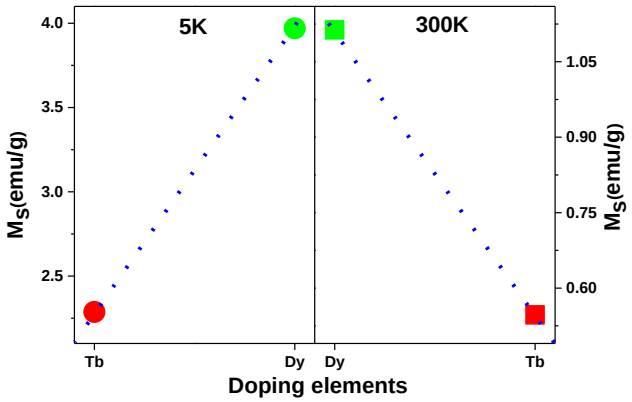

Fig.9 Variation of Saturated magnetisation (M_S) with doping elements in $Bi_{0.8}A_{0.1}Pb_{0.1}Fe_{0.9}Ti_{0.1}O_3$ceramics.

4. Conclusion:

Solid solutions of $(Bi_{0.8}A_{0.1}Pb_{0.1}Fe_{0.9}Ti_{0.1}O_3$ (A = Dy and Tb) confirms thehexagonal structure at room temperature. The dielectric constant measured at frequency= 10 kHz shows Ferroelectric–Paraelectric phase transition at temperature 150–350 ^{0}C.It is observed inparaelectric phase only above Blocking temperature (T_B) i.e. at temperature much higher than T_m.AC conductivity of the material increases with rise intemperature, confirming the Negative Temperature Coefficient of Resistance (NTCR) behaviour of

material.The transformation of paramagnetismto relatively weakanti ferromagnetism in $(Bi_{0.8}A_{0.1}Pb_{0.1}Fe_{0.9}Ti_{0.1}O_3$ (A = Dy and Tb) ceramics due to the influence of the uncompensated anti-ferromagnetic spin. For all these samples, the minor loop traced indicates very weak ferromagnetism associated with anti-ferromagnetic nature.

5. **Conflict of Interest**

Authors declare no conflict of interest.

Acknowledgements

Author Monika Mishra thanks to Registrar Lingaya's Vidyapeeth for providing necessary facilities to carrying out the above research.

References:

[1] M. Fiebig, T. Lottermoser, D. Frohlich, A.V. Goltsev, R.V. Pisarev, Nature, 419 (2002) 818-820.
[2] D.V. Efremov, J. van den Brink, D.I. Khomskii, Nat Mater, 3 (2004) 853-856.
[3] B. Park, S. Hyun, S. Bu, T. Noh, J. Lee, H.-D. Kim, T. Kim, W. Jo, Applied Physics Letters, 74 (1999) 1907.
[4] T.R. Karl, K.E. Trenberth, Science, 302 (2003) 1719-1723.
[5] J. Hemberger, P. Lunkenheimer, R. Fichtl, H.A. Krug von Nidda, V. Tsurkan, A. Loidl, Nature, 434 (2005) 364-367.
[6] J. Xie, C. Feng, X. Pan, Y. Liu, Ceramics International, 40 (2014) 703-706.
[7] V. Singh, S. Sharma, P.K. Jha, M. Kumar, R.K. Dwivedi, Ceramics International, 40 (2014) 1971-1977.
[8] J.S. Kim, C.I. Cheon, P.W. Jang, Y.N. Choi, C.H. Lee, Journal of the European Ceramic Society, 24 (2004) 1551-1555.
[9] G. Catalan, J.F. Scott, Advanced Materials, 21 (2009) 2463-2485.
[10] G. Achenbach, W. James, R. Gerson, Journal of the American Ceramic Society, 50 (1967) 437-437.
[11] H. Schmid, Ferroelectrics, 162 (1994) 317-338.
[12] H. Deng, M. Zhang, Z. Hu, Q. Xie, Q. Zhong, J. Wei, H. Yan, Journal of Alloys and Compounds, 582 (2014) 273-276.
[13] P. Sharma, D. Varshney, S. Satapathy, P.K. Gupta, Materials Chemistry and Physics, 143 (2014) 629-636.
[14] P. Duran, F. Capel, D. Gutierrez, J. Tartaj, M.A. Banares, C. Moure, Journal of Materials Chemistry, 11 (2001) 1828-1836.
[15] R.F. Bhajantri, V. Ravindrachary, A. Harisha, C. Ranganathaiah, G.N. Kumaraswamy, Appl. Phys. A, 87 (2007) 797-805.
[16] W. Shockley, W.T. Read, Jr., Physical Review, 87 (1952) 835-842.
[17] T. Tunç, M. Gökçen, İ. Uslu, Appl. Phys. A, 109 (2012) 649-653.
[18] P. Kumar, M. Kar, Journal of Alloys and Compounds, 584 (2014) 566-572.
[19] W.-M. Zhu, Z.-G. Ye, Applied Physics Letters, 89 (2006) -.
[20] M. Kumar, K.L. Yadav, Journal of Applied Physics, 100 (2006) -.
[21] R. Rai, I. Bdikin, M.A. Valente, A.L. Kholkin, Journal of Advanced Dielectrics, 01 (2011) 257-267.
[22] I. Sosnowska, T.P. Neumaier, E. Steichele, Journal of Physics C: Solid State Physics, 15 (1982) 4835.
[23] E.A. Patterson, D.P. Cann, J. Pokorny, I.M. Reaney, Journal of Applied Physics, 111 (2012) -.
[24] R. Rai, M. Valente, I. Bdikin, A.L. Kholkin, S. Sharma, Solid State Communications, 180 (2014) 56-63.
[25] N. Sahu, M. Kar, S. Panigrahi, Arch Phys Res, 1 (2010) 75-87.
[26] G. Jin, J. Chen, J. Cheng, Ceramics International, (2015).
[27] A.L. Kholkin, I.K. Bdikin, V.V. Shvartsman, N.A. Pertsev, Nanotechnology, 18 (2007) 095502.
[28] R. Rai, M.A. Valente, I. Bdikin, A.L. Kholkin, S. Sharma, Journal of Physics and Chemistry of Solids, 74 (2013) 905-912.
[29] H. Singh, K.L. Yadav, Journal of Alloys and Compounds, 585 (2014) 805-810.
[30] P. Uniyal, K.L. Yadav, Journal of Physics: Condensed Matter, 21 (2009) 012205.
[31] S.B. Kim, S.J. Moon, S.J. Kim, C.S. Kim, Journal of Magnetism and Magnetic Materials, 310 (2007) e592-e594.
[32] Z. Zhou, L. Guo, H. Yang, Q. Liu, F. Ye, Journal of Alloys and Compounds, 583 (2014) 21-31.
[33] R.K. Mishra, D.K. Pradhan, R.N.P. Choudhary, A. Banerjee, Journal of Physics: Condensed Matter, 20 (2008) 045218.
[34] T.-J. Park, G.C. Papaefthymiou, A.J. Viescas, A.R. Moodenbaugh, S.S. Wong, Nano Letters, 7 (2007) 766-772.
[35] D. Kothari, V.R. Reddy, A. Gupta, V. Sathe, A. Banerjee, S.M. Gupta, A.M. Awasthi, Applied Physics Letters, 91 (2007) -.
[36] V.V. Shvartsman, W. Kleemann, R. Haumont, J. Kreisel, Applied Physics Letters, 90 (2007) -.

[37] W. Eerenstein, F.D. Morrison, J. Dho, M.G. Blamire, J.F. Scott, N.D. Mathur, Science, 307 (2005) 1203.

DOI: https://doi.org/10.15379/ijmst.v10i5.3610